ADVANCED MATERIALS TECHNOLOGIES
www.advmattechnol.de

Colloidal Semiconductor Quantum Well Supraparticles as Low-Threshold and Photostable Microlasers

Pedro Urbano Alves, Gemma Quinn, Michael J. Strain, Emek Goksu Durmusoglu, Manoj Sharma, Hilmi Volkan Demir, Paul R. Edwards, Robert W. Martin, Martin D. Dawson, and Nicolas Laurand*

This study introduces and compares the lasing performance of micron-sized and sphere-shaped supraparticle (SP) lasers fabricated through bottom-up assembly of II-VI semiconductor colloidal quantum wells (CQWs) with their counterparts made of quantum dots (CQDs). CQWs consist of a 4-monolayers thick CdSe core and an 8-monolayers thick $Cd_xZn_{1-x}S$ shell with a nominal size of 14 × 15 × 4.2 nm, and CQDs of CdS_xSe_{1-x}/ZnS with 6 nm diameter. SPs are optically characterized with a 0.76 ns pulse laser (spot size: 2.88 × 10^{-7} cm^2) at 532 nm, and emit in the 620–670 nm spectral range. Results show that CQW SPs have lasing thresholds twice as low (0.1–0.3 nJ) as CQD SPs (0.3–0.6 nJ), and stress tests using a constant 0.6 nJ optical pump energy demonstrate that CQW SPs withstand lasing emission for longer than CQD SPs. Lasing emission in CQW and CQD SPs under continuous operation yields half-lives of $\tau_{CQW\,SP}$ ≈150 min and $\tau_{CQD\,SP}$ ≈22 min, respectively. The half-life of CQW SPs is further extended to τ_{QW} ≈385 min when optically pumped at 0.5 nJ. Such results compare favorably to those in the literature and highlight the performance of CdSe-based CQW SPs for laser applications.

1. Introduction

Colloidal semiconductor nanocrystals (NCs) are nanoscale crystals grown via wet chemistry processes and coated with surface ligands that allow them to be suspended in organic solvents.[1,2] According to their size and composition, some NCs can be used as the gain material for novel solution-processed visible lasers when combined with a suitable optical cavity and pumping source.[3,4] Various morphologies of NCs have been investigated for these solution-processed lasers, with the most relevant types being colloidal quantum dots (CQDs) and colloidal quantum wells (CQWs). CQDs are essentially spheroids or cuboids of semiconductor nanocrystals on the scale of a few nanometers that exhibit 3D confinement of electrons and holes.[4,5] On the other hand, CQWs possess slightly elongated dimensions in two directions, with strong confinement occurring only in the third direction. This gives them the characteristic physical aspect of nanosized platelets. Due to this geometry, CQWs tend to exhibit a higher absorption cross-section and a reduced Auger recombination rate compared to CQDs of the same material.[6,7] These features render them advantageous for optically-pumped lasers. Low thresholds for the onset of stimulated emission and high optical gain values have been reported for II-VI Cd-based CQW lasers, enabling the demonstration of

P. U. Alves, G. Quinn, M. J. Strain, M. D. Dawson, N. Laurand
Institute of Photonics
Department of Physics
SUPA
University of Strathclyde
Glasgow G1 1RD, United Kingdom
E-mail: pedro.alves@strath.ac.uk

E. G. Durmusoglu, H. V. Demir
Luminous!
School of Electrical and Electronic Engineering
Nanyang Technological University
Nanyang Avenue 639798, Singapore

The ORCID identification number(s) for the author(s) of this article can be found under https://doi.org/10.1002/admt.202401152

DOI: 10.1002/admt.202401152

M. Sharma
ARC Centre of Excellence in Exciton Science
Department of Materials Science and Engineering
Monash University
Clayton, Victoria 3800, Australia

H. V. Demir
Department of Electrical and Electronics Engineering
Department of Physics
UNAM – Institute of Materials Science and Nanotechnology
Bilkent University
Ankara 06800, Turkey

P. R. Edwards, R. W. Martin
Department of Physics
SUPA
University of Strathclyde
Glasgow G4 0NG, United Kingdom

relatively low laser oscillation thresholds and even lasing under continuous-wave optical pumping.[8,9]

Solution-processed visible lasers have been extensively studied using CQDs or CQWs as gain materials and different geometries as cavities, including Fabry-Perot lasers,[10] microring resonators,[11] vertical cavities implemented with distributed Bragg reflectors,[12] distributed feedback lasers,[13] microsphere resonators[14] and nanobeam photonic crystals.[8]

In 2018, CQDs were simultaneously used as gain material and laser cavities with the demonstration of self-assembled supraparticle (SP) lasers.[15] These SPs, made exclusively from CQDs, are the by-product of an oil-in-water emulsion technique. During the self-assembly process, CQDs come together and form a larger, often partially crystalline structure, with a spherical shape.[16] The structure enables the trapping of light through total internal reflection, ultimately leading to the generation of a whispering gallery mode (WGM) cavity.[16–20] In addition to the unique properties that emerge from self-assembly, the fabrication of these SPs is simple, which makes them accessible for a wide range of applications.

Since 2018, CQD SPs have been the focus of intense research and have been successfully tested as microlasers, with applications including backlight displays,[21] bar-coding,[22] multicolor lasing emission,[18] sensing,[20,23,24] optical coupling and integration into other devices.[25]

Due to the aforementioned features that render CQWs advantageous for optically-pumped lasers, a logical next step would then be the demonstration and study of CQW supraparticle lasers.

The assembly of CQWs into thin film suprastructures of differently-oriented stacks has previously been shown,[26] together with studies on their photoluminescence and amplified spontaneous emission.[12,27] Lasing in SiO_2 microspheres coated with CQW films has also been recently achieved.[28] However, to the authors' knowledge and apart from preliminary work done by our group,[9] the self-assembly of CQW SPs has not been reported yet.

Furthermore, although there has been intense research on NCs for laser applications, the state-of-the-art is lacking studies on the lifespan of microlasers, i.e., the amount of time that they can operate before the brightness of the laser decreases significantly or entirely. The lifespan of a laser is a crucial factor in determining its overall reliability and usefulness in most applications, and a critical factor in applications where the laser must maintain its performance over extended periods. The optical degradation fluence, i.e., the optical pump excitation intensity withstood by the laser over its lifespan, is another parameter of equal importance and capable of providing a more accurate comparison between microlasers that use different optical setups (e.g., setups with optical pumps of different repetition rates or different pump energies).

In this context, this work demonstrates SP lasers made from $CdSe/Cd_xZn_{1-x}$ S CQWs and compares their performance to those of equivalent SP lasers made with CdS_xSe_{1-x}/ZnS CQDs. A comprehensive study is then carried out on the lifespan and optical degradation characteristics of these microlasers compared with other types of Cd-based microlasers covered in the state-of-the-art.

2. Synthesis of SPs

CQD SPs were synthesized from commercial CdS_xSe_{1-x}/ZnS CQDs with an intrinsic emission peak of 625 ± 10 nm (Figure S1, Supporting Information) and a QY of ≈50%, and CQW SPs were synthesized from $CdSe/Cd_xZn_{1-x}S$ core/shell CQWs with an emission peak of 660 ± 10 nm (Figure S1, Supporting Information), and a near-unity QY of 98.5%, which is consistent with the existing literature (see Experimental Section).[7] TEM images of the CQDs and CQWs can be found in Figure S2 (Supporting Information). The synthesis followed an oil-in-water self-assembly process where polyvinyl alcohol (PVA) is used as an emulsifier.[15,16] The first of the two phases consisted of either CQDs or CQWs in chloroform and the second of the two of PVA in MilliQ water. After mixing the two phases, an emulsion was formed. Chloroform was evaporated from the dispersed phase at close to 0 °C to encourage a slow rearrangement and nucleation of the NCs inside the emulsions. The self-assembled SPs were diluted in water at a volume ratio of 1:50 and vortexed again to wash off traces of PVA from their surface. A few microliters of the final solution were drop-cast on a glass slide and left to dry. SPs measured under the microscope were on average 12 ± 3 µm in diameter (Figure S3, Supporting Information).

3. Characterization of SPs

CQW and CQD SPs were characterized individually with a microphotoluminescence (µ-PL) setup (Figure S4, Supporting Information). The setup used a 0.76 ns pulse width microchip laser ($\lambda = 532$ nm) with a repetition rate of 7.1 kHz and a beam spot area of $\approx 2.88 \times 10^{-7}$ cm^2 as the pump source. More details on the optical setup can be found in Supplementary Information (Figure S4, Supporting Information).

The emission intensity versus pump intensity (i.e., the laser transfer function curve) of a CQD SP and CQW SP can be seen in **Figures 1a** and **2a**, respectively. This curve is marked by two distinct regions: the sub-threshold region (left), where spontaneous emission of light occurs (no lasing), and the lasing regime region (right), where stimulated emission of light arises (lasing).

In the sub-threshold region, the output intensity of these SPs increases linearly, and for the CQD SP, it eventually saturates due to Auger recombination. This trend is similar to the typical spontaneous emission behavior observed in optically pumped semiconductor NCs. At the lasing threshold (≈0.3 nJ for the CQD SP in Figure 1, and 0.1 nJ for the CQW SP in Figure 2), the slope changes dramatically and the SPs enter the lasing regime region. The lasing regime of these SPs is characterized by the linear proportionality between the pump input energy and the laser output. Under these conditions, SPs work as a pump-to-light converter with a conversion efficiency given by the slope, γ.

The dashed lines fit to the spontaneous emission[25] and lasing emission (linear regression) observed below and above the laser threshold, respectively (Figures 1b,2b). The transition to the lasing regime can also be observed under the microscope, where the whispering gallery modes characteristic of spherical cavities in CQD and CQW SPs become noticeable (Figures 1c and 2c, respectively). Further characterization using a scanning electron microscope (SEM) shows the morphology of these SPs (Figures 1c and 2c).

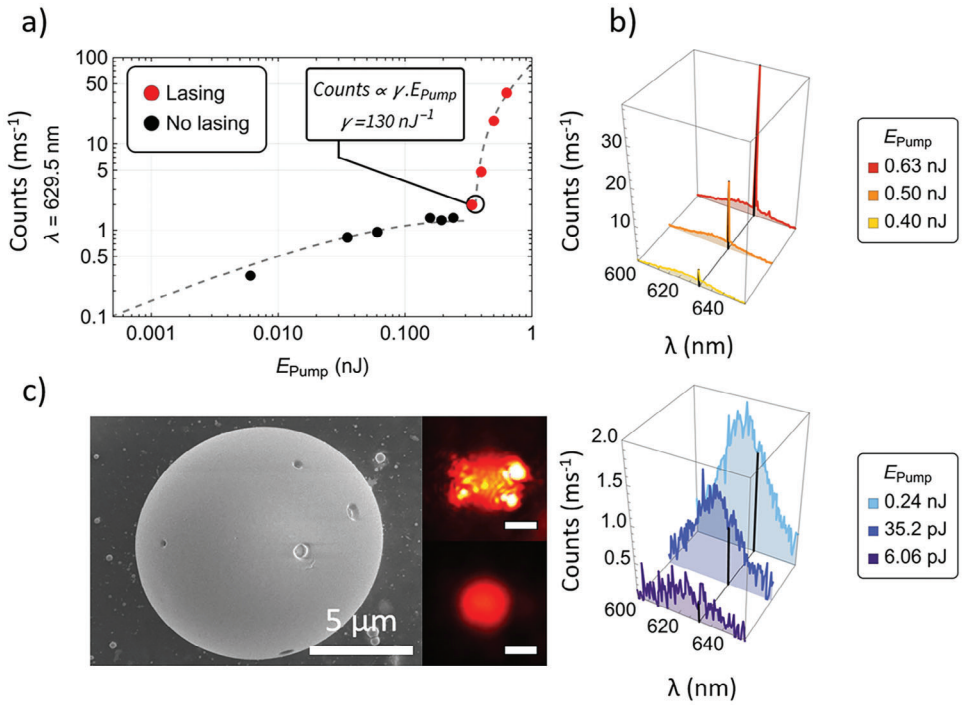

Figure 1. Optical characterization of a quantum dot supraparticle: Laser transfer function curve ($\lambda = 629.5$ nm) of CQD SP (1) with 9 µm diameter a), together with its photoluminescence b) below (bottom graph) and above (top graph) laser threshold. The dark lines in the photoluminescence spectra indicate the data points extracted at $\lambda = 629.5$ nm and used to plot the laser transfer function curve. The typical morphology of a drop cast CQD SP can be seen in the scanning electron micrograph c), together with optical micrographs of the characterized SP below (bottom) and above (top) laser threshold.

Overall and for SPs of similar sizes, CQW SPs outperformed their CQD counterparts with laser thresholds twice as low (Figures S5 and S6, Supporting Information). This difference is mainly attributed to the properties of the different types of NCs, but there are also other factors affecting the laser threshold (e.g., pump spot size, density of NCs in the SP, Q-factor, and size of the SP).[25] Below the lasing threshold, under the same optical pump conditions, and for SPs of the same size, the count rate was ≈2× higher for CQW SPs. This count rate ratio is similar to the quantum yield (QY) ratio between CQWs and CQDs in solution ($\frac{98.5\%}{50\%} = 2.0$, see Experimental Section). From the extracted data it is also noticeable that the sub-threshold region of CQD SPs reaches a distinct plateau (Figure 1a), whereas the sub-threshold region of CQW SPs transitions to the lasing regime without such a pronounced plateau (Figure 2a). The lack of a pronounced plateau in CQW SPs is indicative of efficient radiative recombination and non-dominant non-radiative recombination.[29]

The difference between CQD SPs and CQW SPs is also reflected in the lasing regime, where the light conversion efficiency in a millisecond becomes more than an order of magnitude higher in CQW SPs ($\frac{2300\ counts.nJ^{-1}}{130\ counts.nJ^{-1}} = 17.7$; Figure 2a vs Figure 1a). CQD SPs and CQW SPs showed multimode emission (Figures S7 and S8, Supporting Information) and had estimated Q-factors between 330 and 350 (Figures S9 and S10, Supporting Information, respectively). The Q-factor for CQD SPs is consistent with those reported in the literature.[15]

Similarly to CQD SPs, the transition to the lasing regime in CQW SPs could also be observed under the microscope (Figure 2c). Despite the different natures in shape between CQDs and CQWs, no noticeable differences in the morphology of CQW SPs were observed under SEM at the µm scale (Figure 2c).

4. Lifespan of SP Lasers

The lasing lifespan studies on CQD and CQW SPs were performed by optically pumping the SPs above the laser threshold (0.6 nJ, or 2.2 mJ cm^{-2}) for the duration of the experiment (i.e., 60 min), and by acquiring the spectra at intervals of 1 min. From this, a density plot of the emission wavelength versus time was generated for each SP. This experiment comprised the study of 2 sets of 2 SPs each. The first set includes one CQW SP and one CQD SP of 9 µm diameter each (i.e., CQW SP (1) and CQD SP (1) optically characterized in the previous section), and the second set includes one CQW SP and one CQD SP of 14 µm diameter each (i.e., CQW SP (2) and CQD SP (2), with optical characterization in Figures S11 and S12, Supporting Information). **Figure 3** shows the lasing emission spectra of the two sets, with spectrometer resolution-limited (0.7 nm) peaks between 625 nm and 645 nm for CQD SPs and 670 nm and 690 nm for CQW SPs. Larger SPs (CQW SP(2) and CQD SP (2), Figure 3) show a higher number of lasing modes compared to the smaller SPs (CQW SP(1) and CQD SP (1), Figure 3) due to their smaller free spectral range (FSR).[30] It is also worth noting that the resonant wavelengths inside the cavity (WGMs) of the SPs depend on the size,

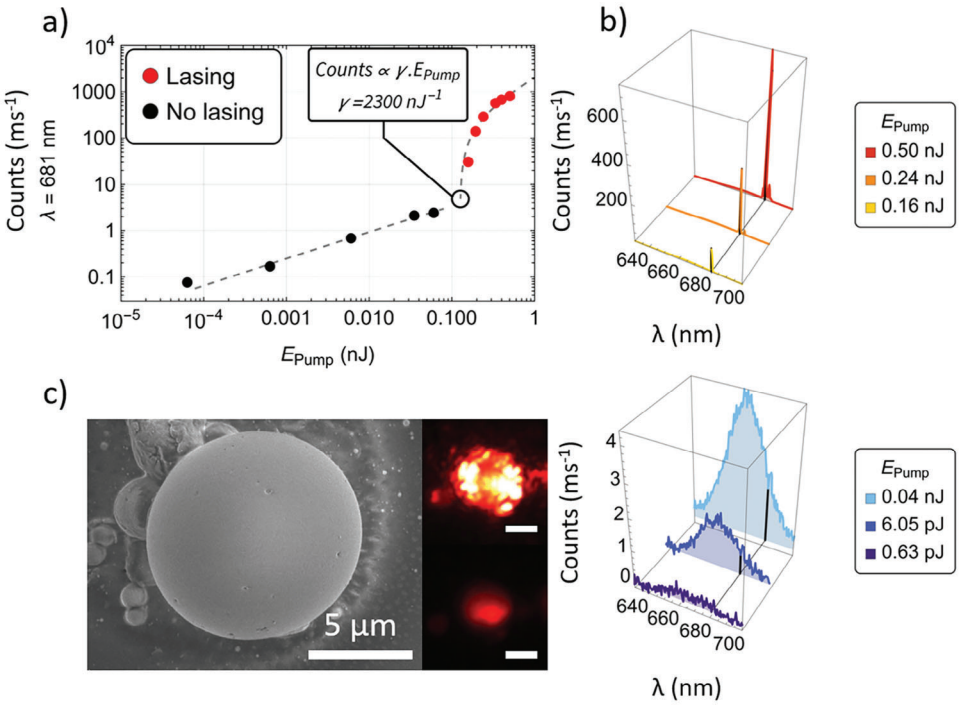

Figure 2. Optical characterization of a quantum well supraparticle: Laser transfer function curve ($\lambda = 681$ nm) of CQW SP (1) with 9 µm diameter a), together with its photoluminescence b) below (bottom graph) and above (top graph) laser threshold. The dark lines in the photoluminescence spectra indicate the data points extracted at $\lambda = 681$ nm and used to plot the laser transfer function curve. The typical morphology of a random drop cast CQW SP can be seen in the scanning electron micrograph c), together with optical micrographs of the characterized SP below (bottom) and above (top) laser threshold.

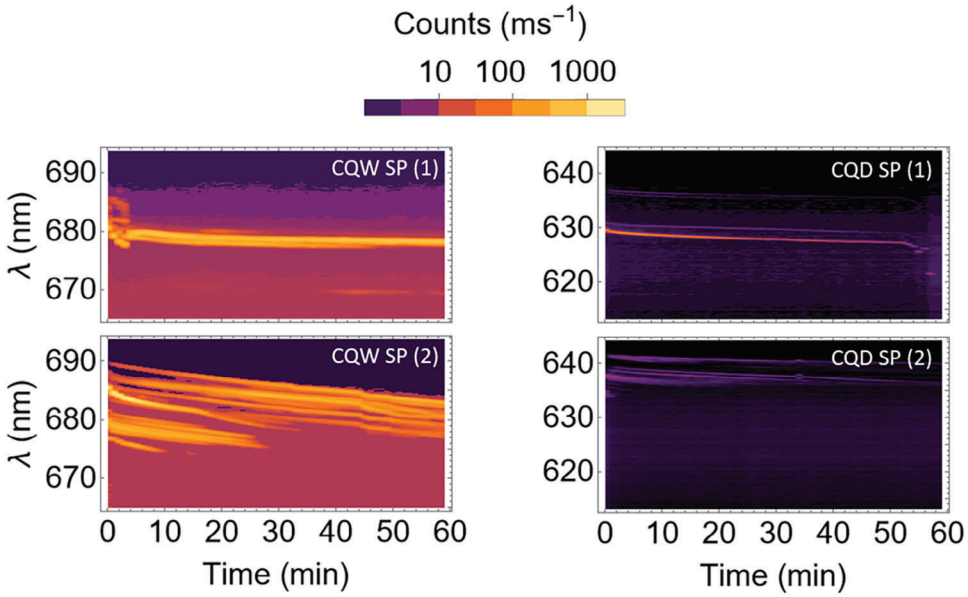

Figure 3. Density plots of the characterized NC SPs, show the evolution of the lasing modes as a function of time under continuous optical pumping at 2.2 mJ cm^{-2}. The two plots on the left correspond to CQW SPs with 9 (1) and 14 µm (2) in diameter. The two plots on the right correspond to CQD SPs with 9 (1) and 14 µm (2) in diameter.

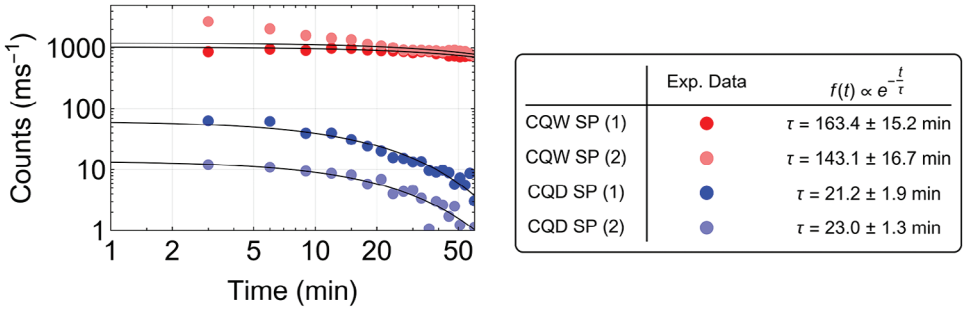

Figure 4. Laser lifespan in CQD and CQW SPs. The counts on the spectrometer corresponding to the lasing peaks have been plotted as a function of elapsed time and fitted to an exponential decay function $f(t)$. The estimated τ (half-life) was ≈150 min for CQW SPs and 22 min for CQD SPs.

overall refractive index, and shape (spherical-shaped or spheroid-shaped) of the SPs.[30] In both sets of SPs, shifts in the wavelength of the lasing peaks were observed over time. These shifts could be mainly attributed to the photodegradation of SPs.[31–33]

The lifespan of these microlasers in the lasing regime was then estimated by extracting the counts of the lasing modes from the PL spectra. The lifespan of SPs was gauged by fitting the extracted counts to an exponential decay and finding the half-life values.[34] **Figure 4** shows the extracted data for each of the four SPs and their fitted half-life times. CQD SPs had an estimated half-life of ≈22 min, an order of magnitude lower than the estimated half-life for CQW SPs (150 min). These results show a higher resistance to optical degradation from CQWs when compared to CQDs.

Photo-activation and degradation (i.e., enhancement and decay of PL emission) have been reported in NCs through several processes (e.g., charged defect passivation, ligand stabilization, photo annealing, or light-assisted adsorption of water).[32] While a moderate exposure to light can contribute to the removal of excess ligands in NCs, smoothen the surface defects by photo-adsorption, and promote photo-activation, long and intense exposures to light will result in exaggerated smoothing and eventual etching of the NCs leading to additional trap states and ultimately photodegradation.[32,33]

The capture of carriers by trap states (photocharging) has been reported to decrease the refractive index in CQDs, and therefore this reduction is also likely to happen in CQD SPs.[33] Under constant photoexcitation, photocharging appears to be dominant and is sufficient to blue shift the lasing modes of both CQD[33] and CQW SPs over time as seen in Figure 3.

Photodegradation processes can also increase the refractive index. The loss of ligands in CQDs has been reported to lead to a densification of the CQDs in films, which causes a red shift in their emission and an increase in their refractive index.[32,35] If such an effect is present in the SPs here it should be negligible compared to photocharging given the blue shift of the lasing wavelengths. Still, one can look for it through the analysis of the non-lasing part of the PL. Any decrease in the non-lasing PL would also be an additional, indirect indicator of the formation of non-radiative surface traps via photo-oxidation and erosion on the surface of NCs upon long irradiation times.[33] Similarly to what has been reported for CQD SPs,[33] signs of photo annealing and photodegradation over time are also present in the CQD and CQW SPs studied here, such as the initial decrease in the non lasing PL emission (Figure S13, Supporting Information) and minimal shifts in the PL peak over time (Figure S14, Supporting Information). The longer lifespan of lasing modes in CQW SPs suggests that photodegradation happens faster for CQD SPs.

The elapsed time of the four SPs under continuous operation for 60 min can be visually observed in Supplementary Information (Video S1, Supporting Information).

5. Lifespan of CQW SP Lasers under Low-Excitation

To study if the lifespan of CQW SPs could be extended by lowering the optical pump fluence to values closer to their laser threshold, a third CQW SP (CQW SP (3), **Figure 5**) with a diameter of 18 µm (Figure S3, Supporting Information) was optically excited at 0.5 nJ (1.7 mJ cm^{-2}) during 90 min. This CQW SP had a laser threshold of ≈0.16 nJ (Figure S15, Supporting Information) and a Q-factor of ≈350 (Figure S16, Supporting Information). From its laser spectrum density plot (Figure 5a), the reduction in the optical pump fluence from 0.6 nJ (2.2 mJ cm^{-2}) to 0.5 nJ (1.7 mJ cm^{-2}) showed an increase in the stability of the lasing modes. The negligible variations in wavelength and intensity of the lasing modes throughout the experiment indicate a marked decrease in the degradation of the SP. This stability can also be observed in the laser lifespan measurements (Figure 5b), where the estimated half-life time of the CQW SP was increased from 150 to 385 min.

6. Optical Regeneration of SP Lasers

A final study was carried out to determine the regeneration capabilities of these lasers. For this purpose, CQW SP (1) previously characterized in Figure 3 was left to rest for 1 h and 30 min, and optically excited for another 10 min at under 2.2 mJ cm^{-2}. Inspection of the laser spectrum density results shows that the lasing modes resumed at approximately the same wavelengths where the experiment had stopped (**Figure 6a**) and the extracted data showed no signs of regeneration. These results are consistent with the photodegradation processes previously discussed in the lifespan of SPs, where the permanent damage caused to the organic ligands is not recoverable in these NCs.[31]

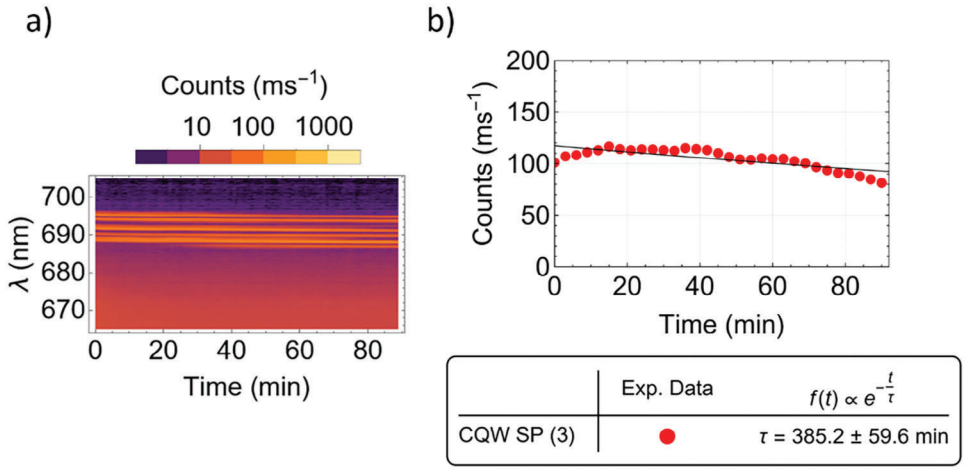

Figure 5. Laser spectrum density plot of a CQW SP with 18 µm diameter under continuous optical pumping over 90 min at 1.7 mJ cm^{-2} a) and its estimated half-life b), with $\tau = 385$ min.

7. CQW SP Lasers Versus State of Art

Table 1 presents a collection of studies found in the literature on CdSe-based NC microlasers reporting lifespan measurements. Flexible distributed feedback (DFB) lasers using CdSe colloidal CQDs have reported lifespans with a half-life of ≈10 min.[36] Vertical cavity surface emitting microlasers (VCSELS) using thin films of CdSe CQDs have shown a half-life of 2.4×10^3 min.[37] Studies on coated and uncoated thin films of neat CdSe-based CQDs optically pumped by a stripe-shaped beam have reported maintaining the optical gain regime required for lasing for a half-life of 10^1–10^2 min.[38] **Figure 7** shows the optical degradation of these devices (degradation fluence = pump fluence × rep. rate × laser lifespan), where all the results based on thin layers of neat CQDs are shown to fall within 10^4 and 10^6 mJ cm^{-2}. State-of-the-art studies on CdSe-based CQD SPs include half-lives of ≈50 min (Table 1) and optical degradation thresholds in the order of 10^7 mJ cm^{-2} (Figure 7).[39]

The results in this work on CdSe-based CQD SPs have shown a half-life of ≈22 min (Table 1) and degradation fluences between 10^7 and 10^8 mJ cm^{-2} (Figure 7), consistent with the findings in the state-of-the-art.[39]

The novel CdSe-based CQW SPs have shown half-lives between 10^2 and 10^3 min and their degradation fluence (≈2•10^8 mJ cm^{-2}) was similar regardless of the optical pump energy (see Table 1). CQW SPs had the 2nd highest half-life (after VCSELs) and degradation values that surpassed those of all the CdSe-based CQD devices here reported and found in the literature by at least 1 order of magnitude (Figure 7).

8. Conclusion

This work demonstrated lasing in CQW SPs and compared their performance (i.e., laser threshold and lifespan in the lasing regime) to the performance of CQD SPs. The comparison between CQW SPs and CQD SPs has shown that CQW SPs

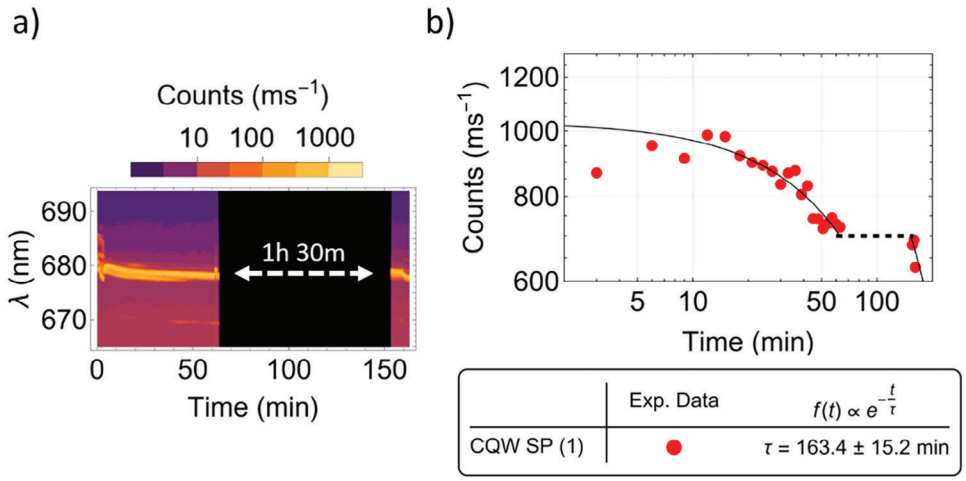

Figure 6. Study on the regeneration capabilities of SP NCs using CQW SP (1) as a model (9 µm in diameter). The CQW SP was left to rest for 1 h and 30 min and optically pumped again under 2.2 mJ cm^{-2} for another 10 min. The laser density plot a) shows that lasing modes resumed at approximately the same wavelength. However, the SP did not show any signs of regeneration as the exponential decay fitted trend continued from where it was left (b).

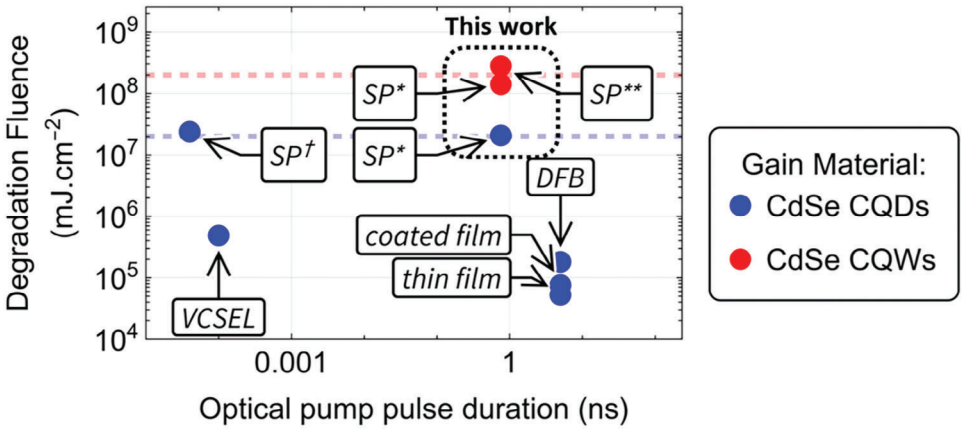

Figure 7. Degradation fluence of CdSe-based microlasers versus the optical pump pulse duration. This figure comprises data found in the literature with data from the studies in this paper. The specifications of each microlaser can be found in Table 1. Spherical resonators include SPs in the state-of-the-art (SP†) and the SPs presented in this work (SP* and SP**).

exhibit a better performance overall, with an expected half-life in the lasing regime (at high optical pump fluence: 2.2 mJ cm^{-2}) of 150 min for CQW SPs, versus the 22 min for CQD SPs. The lifespan expectancy of CQW SPs was further extended by operating these devices at decreased optical pump fluences (1.7 mJ cm^{-2}). This decrease in pump fluence led to a half-life of ≈385 min in CQW SPs, which corresponds to more than twice the recorded life-time at high optical pump fluence. CQW SPs were also used as a subject of study to verify if SP lasers have regeneration capabilities. However, a cooldown period of 1 h and 30 min showed no signs of optical recovery in laser intensity. This was attributed to photodegradation in colloidal NCs, where the thermal build-up of long and continuous operation times causes permanent damage.[31–33] Nevertheless, the results here recorded for CdSe-based CQD and CQW SPs have shown optical degradation fluences orders of magnitude higher than those reported in the state-of-the-art for other CdSe-based microlasers and thin films. In particular, CQW SPs recorded the highest optical degradation fluences, at least one order of magnitude higher than the other CdSe-based microlasers. The comparison between CQW SPs and the other microlasers in the state-of-the-art in terms of lifespan in the lasing regime and optical degradation highlights their overall superior performance. This paves the way for the use of CQW SPs in optical applications where laser durability and stability are a requirement.

9. Experimental Section

Chemicals: Toluene (anhydrous, 99.8%) and polyvinyl alcohol (average Mw 85000–124000, 87–89% hydrolyzed) were supplied by Merck and used as received. Water was purified with a Milli-Q water purification system.

Quantum Dots: Cadmium selenide sulfide (core) zinc sulfide (shell) fluorescent CQDs with an emission wavelength of 625 ± 10 nm (Figure S1, Supporting Information), diameter of 5.5–6.5 nm and QY of ≈50% were supplied by CDBioparticles (Cat.No: DNP-C006, CDBioparticles, New York).

Quantum Wells: The CQWs were synthesized[7] and were ≈14 × 15 nm in width × length. They consisted of a CdSe core 4 monolayers thick and a CdS shell ≈8 monolayers thick synthesized by the hot-injection shell growth method. The emission peak of individual CQWs was centered at 660 ± 10 nm (Figure S1, Supporting Information). CQWs exhibited a near-unity (98.5%) QY, which is in agreement with the existing literature.[7]

Synthesis of Supraparticles: The self-assembly of SPs followed an oil-in-water emulsion prepared at room temperature. Two immiscible solutions were prepared, one with the NCs dissolved in toluene at a concentration

Table 1. CdSe-based colloidal NC microlasers and the state-of-the-art on their lifespan, including the details on the type of laser and excitation source. Spherical resonators include SPs in the state-of-the-art (SP†) and the SPs here presented (SP* and SP**).

Microlaser			Optical excitation source			
Cavity	Estimated laser lifespan [min]	Gain material (CdSe NC)	Pump λ [nm]	Pulse width [ns]	Repetition rate [Hz]	Pump fluence [mJ cm^{-2}]
DFB[36]	9.4	QD	355	5	10	6.0
Spherical SP†[39]	4.8×10^{1}	QD	400	40×10^{-6}	10 000	0.2
VCSEL[37]	2.4×10^{3}	QD	400	100×10^{-6}	1000	3.3×10^{-3}
Thin film (no cavity)[38]	5.8×10^{1}	QD	355	5	10	1.5
Coated film (no cavity)[38]	8.4×10^{1}	QD	355	5	10	1.5
Spherical SP*	2.2×10^{1}	QD	532	0.76	7100	2.2
Spherical SP*	1.5×10^{2}	QW	532	0.76	7100	2.2
Spherical SP**	3.9×10^{2}	QW	532	0.76	7100	1.7

of 250 mg ml^{-1}, and another with PVA dissolved in milli-Q water at a mass ratio of 1.25%. The emulsion was prepared by vortexing 115 µl of the NC solution with 450 µl of the water solution for 10 min and stirring the mixture for ≈2 h at 750 rpm and in an ice bath close to 0 °C. Once the stirring was completed, self-assembled SPs were diluted in water at a volume ratio of 1:50 and vortexed again to remove traces of PVA from their surface. Samples in this work were prepared by drop-casting 10 µl of cleaned SPs onto a glass substrate.

Optical Characterization of NCs: The PL of NCs in solution was measured in a 1 × 1 cm microcuvette. The microcuvette was placed in a 4-port cuvette holder (Thorlabs, CVH100) and a 532 nm laser (Thorlabs, 532 nm DPSS, DJ532- 10) with an optical output power of 10 mW was used to excite each sample. The PL measurements were done at 90 degrees to the laser diode to avoid interference from the excitation source and used a spectrometer (Ocean Optics, USB 4000; resolution: 2 nm at full-width half maximum) to collect the PL spectrum of NCs in solution. The absorbance spectrum was measured on these same samples using a spectrophotometer (Thermo Scientific, GENESYS 30 Visible Spectrometer). More information on the absorption and PL spectra of NCs can be found in (Figure S1, Supporting Information).

Optical Characterization of SPs: The PL and absorbance measurements on SPs followed the same procedure as the NCs in solution (Figure S1, Supporting Information). The PL measurements for the laser transfer function and laser lifespan of SPs were performed on the optical setup in Figure S4 (Supporting Information). The SPs were optically pumped with a 0.76 ns pulse width microchip pulsed laser ($\lambda = 532$ nm, MNG-03E-100, Teem Photonics) at a repetition rate of 7.1 kHz and with a beam spot area of $\approx 2.88 \times 10^{-7}$ cm^2 for the individual characterization. The beam was attenuated with a variable wheel attenuator and focused on the sample with an objective lens (4×/ NA 0.13, Nikon). A spectrometer (AvaSpec-2048-4-DT, Avantes) with a 0.7 nm spectral resolution between 220–1100 nm was used to acquire the spectrum data. A power meter was used to calibrate the output energy as a function of the attenuator filter before each experiment. More details on the setup can be seen in (Figure S4, Supporting Information).

SEM Characterization: A FEI Sirion 200 field-emission gun scanning electron microscope (FEG-SEM) was used to acquire images of the SP morphology. The secondary electron signal was used for the images presented in this work.

Supporting Information

Supporting Information is available from the Wiley Online Library or from the author.

Acknowledgements

The author acknowledge support from the Leverhulme Trust for the Research Leadership Award RL-2019-038. This research is also supported by the Singapore Agency for Science, Technology, and Research (A*STAR) MTC program, Grant No. M21J9b0085 and the Ministry of Education, Singapore, under its Academic Research Fund Tier 1 (MOE-RG62/20), and by the TUBITAK 119N343, 120N076, 121N395, and 20AG001. Hilmi Volkan Demir also acknowledges the support from the TUBA and TUBITAK 2247-A National Leader Researchers Program (121C266).

Conflict of Interest

The authors declare no conflict of interest.

Data Availability Statement

The data that support the findings of this study are openly available in https://www.re3data.org/repository/r3d100012412 at https://doi.org/10.15129/c8a8f5ea-3878-4d15-83ed-ddcca1477706, reference number 184080573.

Keywords

lasers, micro resonators, nanocrystals, optical devices, quantum dots, quantum wells, self-assembly

Received: July 17, 2024
Published online: August 8, 2024

[1] A. M. Smith, S. Nie, *Acc. Chem. Res.* **2010**, *43*, 190.
[2] D. V. Talapin, J. S. Lee, M. V. Kovalenko, E. V. Shevchenko, *Chem. Rev.* **2010**, *110*, 389.
[3] V. I. Klimov, *Annu. Rev. Phys. Chem.* **2007**, *58*, 635.
[4] Y. S. Park, J. Roh, B. T. Diroll, R. D. Schaller, V. I. Klimov, *Nat. Rev. Mater.* **2021**, *6*, 382.
[5] H. Jung, N. Ahn, V. I. Klimov, *Nat. Photonics* **2021**, *15*, 643.
[6] Y. Altintas, B. Liu, P. L. Hernández-Martínez, N. Gheshlaghi, F. Shabani, M. Sharma, L. Wang, H. Sun, E. Mutlugun, H. V. Demir, *Chem. Mater.* **2020**, *32*, 7874.
[7] Y. Altintas, K. Gungor, Y. Gao, M. Sak, U. Quliyeva, G. Bappi, E. Mutlugun, E. H. Sargent, H. V. Demir, *ACS Nano* **2019**, *13*, 10662.
[8] Z. Yang, M. Pelton, I. Fedin, D. V. Talapin, E. Waks, *Nat. Commun.* **2017**, *8*, 143.
[9] P. U. Alves, M. Sharma, E. G. Durmusoglu, M. Izmir, M. D. Dawson, H. V. Demir, N. Laurand, in *2022 IEEE Photonics Conference, IPC 2022 – Proceedings*, IEEE, New Jersey, USA **2022**.
[10] C. Dang, J. Lee, C. Breen, J. S. Steckel, S. Coe-Sullivan, A. Nurmikko, *Nat. Nanotechnol.* **2012**, *7*, 335.
[11] B. Le Feber, F. Prins, E. De Leo, F. T. Rabouw, D. J. Norris, *Nano Lett.* **2018**, *18*, 1028.
[12] B. Guzelturk, Y. Kelestemur, M. Olutas, S. Delikanli, H. V. Demir, *ACS Nano* **2014**, *8*, 6599.
[13] M. M. Adachi, F. Fan, D. P. Sellan, S. Hoogland, O. Voznyy, A. J. Houtepen, K. D. Parrish, P. Kanjanaboos, J. A. Malen, E. H. Sargent, *Nat. Commun.* **2015**, *6*, 6.
[14] Z. Yuan, Z. Wang, P. Guan, X. Wu, Y. -C. Chen, *Adv. Opt. Mater.* **2020**, *8*, 1901596.
[15] F. Montanarella, D. Urbonas, L. Chadwick, P. G. Moerman, P. J. Baesjou, R. F. Mahrt, A. Van Blaaderen, T. Stöferle, D. Vanmaekelbergh, *ACS Nano* **2018**, *12*, 12788.
[16] E. Marino, E. Marino, A. W. Keller, D. An, S. Van Dongen, S. Van Dongen, T. E. Kodger, K. E. MacArthur, M. Heggen, C. R. Kagan, C. R. Kagan, C. R. Kagan, C. B. Murray, C. B. Murray, P. Schall, *J. Phys. Chem. C* **2020**, *124*, 11256.
[17] E. Marino, A. Sciortino, A. Berkhout, K. E. MacArthur, M. Heggen, T. Gregorkiewicz, T. E. Kodger, A. Capretti, C. B. Murray, A. Femius Koenderink, F. Messina, P. Schall, *ACS Nano* **2020**, *14*, 13806.
[18] P. U. Alves, N. Laurand, M. D. Dawson, *2020 IEEE Photonics Conference, IPC 2020 – Proceedings*, IEEE, New Jersey, USA **2020**, 20.
[19] P. U. Alves, D. Jevtics, M. J. Strain, M. D. Dawson, N. Laurand, *2021 IEEE Photonics Conference, IPC 2021 – Proceedings*, IEEE, New Jersey, USA **2021**, 2021.
[20] K. H. Kim, P. H. Dannenberg, H. Yan, S. Cho, S. H. Yun, *Adv. Funct. Mater.* **2021**, *31*, 2103413.
[21] W. Chen, L. Wang, R. Liu, H. Shen, J. Du, F. Fan, *Nano Lett.* **2023**, *23*, 437.
[22] A. R. Anwar, M. Mur, M. Humar, *ACS Photonics* **2023**, *10*, 1202.
[23] X. Yang, C. Gong, C. Zhang, Y. Wang, G. F. Yan, L. Wei, Y. C. Chen, Y. J. Rao, Y. Gong, *Laser Photon Rev* **2022**, *16*, 2100171.
[24] N. Toropov, G. Cabello, M. P. Serrano, R. R. Gutha, M. Rafti, F. Vollmer, *Light Sci Appl* **2021**, *10*, 42.

[25] P. U. Alves, B. J. E. Guilhabert, J. R. McPhillimy, D. Jevtics, M. J. Strain, M. Hejda, D. Cameron, P. R. Edwards, R. W. Martin, M. D. Dawson, N. Laurand, *ACS Applied Optical Materials* **2023**, *1*, 1836.
[26] O. Erdem, K. Gungor, B. Guzelturk, I. Tanriover, M. Sak, M. Olutas, D. Dede, Y. Kelestemur, H. V. Demir, *Nano Lett.* **2019**, *19*, 4297.
[27] M. Sharma, S. Delikanli, H. V. Demir, Proceedings of the IEEE, IEEE, New Jersey, USA **2020**, 655.
[28] Y. T. Thung, R. Duan, E. G. Durmusoglu, Y. He, L. Xiao, C. X. X. Lee, W. S. Lew, L. Zhang, H. V. Demir, H. Sun, *Laser Photon Rev* **2023**, *17*, 2200849.
[29] A. Brumberg, N. E. Watkins, B. T. Diroll, R. D. Schaller, *Nano Lett.* **2022**, *22*, 6997.
[30] G. C. Righini, Y. Dumeige, P. Féron, M. Ferrari, G. N. Conti, D. Ristic, S. Soria, *Rivista del Nuovo Cimento* **2011**, *34*, 435.
[31] P. N. Goswami, D. Mandal, A. K. Rath, *Nanoscale* **2018**, *10*, 1072.
[32] E. Moyen, A. Kanwat, S. Cho, H. Jun, R. Aad, J. Jang, *Nanoscale* **2018**, *10*, 8591.
[33] S. J. Neuhaus, E. Marino, C. B. Murray, C. R. Kagan, *Nano Lett.* **2023**, *23*, 645.
[34] I. Wolfram, Mathematica, Version 14.1 Wolfram Research, Inc, Champaign, IL **2024**.
[35] B. T. Diroll, E. A. Gaulding, C. R. Kagan, C. B. Murray, *Chem. Mater.* **2015**, *27*, 6463.
[36] Y. Chen, B. Guilhabert, J. Herrnsdorf, Y. Zhang, A. R. MacKintosh, R. A. Pethrick, E. Gu, N. Laurand, M. D. Dawson, in *Proceedings of the IEEE Conference on Nanotechnology*, IEEE, New Jersey, USA **2011**, 958.
[37] L. Zhang, H. Yang, Y. Tang, W. Xiang, C. Wang, T. Xu, X. Wang, M. Xiao, J. Zhang, *Chem. Eng. J.* **2022**, *428*, 131159.
[38] L. J. Mclellan, *Colloidal Quantum Dot and Hybrid Lasers*, University of Strathclyde, Glasglow, UK **2018**.
[39] H. Chang, Y. Zhong, H. Dong, Z. Wang, W. Xie, A. Pan, L. Zhang, *Light Sci Appl* **2021**, *10*, 60.